



Physical properties of W_2GaX ($X=C, N$, and F) based novel MAX phases; potential materials for applications in advanced electronic and optical devices

Bakhtiar Ul Haq^{a,*}, Se-Hun Kim^{a,b,*}, R. Ahmed^{c,d}, Aijaz Rasool Chaudhry^e, Muhammad Shabbir^{f,g}, A. Laref^h

^a Faculty of Science Education, Jeju National University, Jeju 63243, Republic of Korea

^b Department of Physics, Faculty of Science, King Khalid University, P.O. Box 9004, Abha, Saudi Arabia

^c Center for High Energy Physics, University of the Punjab, Quaid-e-Azam Campus Lahore-54590, Pakistan

^d Department of Physics, Faculty of Science, Universiti Teknologi Malaysia, UTM, Skudai 81310 Johor, Malaysia

^e Department of Physics, College of Science, University of Bisha, P.O. Box 551, Bisha 61922, Saudi Arabia

^f Department of Chemistry, Faculty of Science, King Khalid University, P.O. Box 9004, Abha 61413, Saudi Arabia

^g Research Center for Advanced Materials Science (RCAMS), King Khalid University, P.O. Box 9004, Abha 61413, Saudi Arabia.

^h Department of Physics and Astronomy, College of Science, King Saud University, Riyadh 11451, Saudi Arabia

ARTICLE INFO

Keywords:

MAX phases
 W_2GaX
First principles approach
Cohesive energy
Electronic structure
Absorption coefficients

ABSTRACT

This study examines the electronic and optical characteristics of W_2GaX ($X = C, N$, and F) MAX phases using first-principles approach. The cohesive energies of W_2GaC , W_2GaN , and W_2GaF are determined as 7.31, 6.40, and 5.05 eV, respectively, demonstrating excellent agreement with existing literature and confirming their stability. The $W-d$, $Ga-s$, and $X-p$ states are symmetrically dispersed across the spin-polarized electronic structures, resulting in a nonmagnetic metallic behavior of W_2GaX . Due to their metallic behavior, they reflect more than 60 % of infrared and up to 50 % of visible light. These compounds demonstrate considerable absorption of infrared, visible, and ultraviolet (UV) light, with absorption coefficients of approximately $\sim 10^4 \text{ cm}^{-1}$, $\sim 10^5 \text{ cm}^{-1}$, and $\sim 10^6 \text{ cm}^{-1}$, respectively. The refractive indices of W_2GaX MAX phases remain greater than one for incident light energies below 10 eV. Additionally, W_2GaC shows the highest optical conductivity among the investigated compounds when exposed to light, making it a promising material for various conduction applications. Our present study sheds light on the optical and electronic properties of W_2GaX MAX phases and highlights their potential for applications in advanced electronic and optical devices.

1. Introduction

MAX phases refer to a collection of nanolaminate compounds that maintain thermodynamic stability, and are represented by a generic chemical formula $M_{n+1}AX_n$. M , A , and X are the Transition metals, Group-A members, and Carbon or Nitrogen [1]. The constituting M , A , and X atoms govern the behaviour of the MAX phases. Similarly, integer n in the formula $M_{n+1}AX_n$ plays a prominent role in classifying MAX phases. For instance, for $n = 1, 2, 3$, the MAX phases have been classified into subclasses such as M_2AX , M_3AX_2 , and M_4AX_3 [2]. The MAX phases exhibit hexagonal crystal symmetry where bonds of metallic nature associate the M and A atoms. In contrast, M and X atoms are attached by covalent bonds. Within the unit cell, the M and X atoms are arranged in

$M_{n+1}X_n$ octahedra sandwiched between the A atomic layers. Hence, these $M_{n+1}X_n$ octahedra and A atomic layers are arranged in a vertically stacked $M-A-M-X-M-A-M-X$ sequence along c -axis [3].

All the MAX phases are of metallic nature owing to the existence of metallic bonds among the M and A atoms that make them electrically conductive. The metallic bonding between the M and A atoms is due to the presence of partially filled d -orbitals in the M atoms close to the Fermi level [3–5]. In addition to their metallic nature, they display ceramic behavior as they are synthesized at high temperatures from metal and nonmetal atoms [3]. The simultaneous ceramic and metallic nature and high mechanical and thermal stability, make these compounds resistant to thermal shock, oxidation, creep, and corrosion and have found reliable applications in harsh conditions [6–9]. Due to these

* Corresponding authors.

E-mail addresses: bakhtiar@jejunu.ac.kr (B. Ul Haq), spinjj@jejunu.ac.kr (S.-H. Kim).

<https://doi.org/10.1016/j.comptc.2023.114427>

Received 22 September 2023; Received in revised form 22 November 2023; Accepted 2 December 2023

Available online 4 December 2023

2210-271X/© 2023 Elsevier B.V. All rights reserved.

exciting features, they have been used as high-temperature ceramics, tribological components, gas burner nozzles, concrete's dry drilling, protective coatings, electrical contacts for catalysis, applications in sensors as well as alternate of graphite for high-temperature applications [10–27]. Therefore, they have received significant interest from researchers where around 60 compounds of the MAX phases have already been synthesized, and more than 150 additional stable MAX phases have been identified [25–29]. Moreover, the MAX phases are no longer confined solely to ternary carbides and nitrides; they now encompass ternary borides as well [30]. The applications of the MAX phases have been further extended to the field of spintronics with the recent discovery of magnetic MAX phases [31–33].

The existing literature on MAX phases highlights a significant correlation between their physical properties and the comprising metallic and nonmetallic components [31–33]. These properties can be effectively modulated through controlled changes in the constituents. A recent study synthesized a new stable quaternary *i*-MAX based on Tungsten (W) in this quest [34]. However, to our knowledge, no thorough investigations into the physical properties of W_2GaX , have been carried out up to date. For this reason, the physical characteristics of W_2GaX are carefully examined in this study. We discuss in detail its optical spectra, electronic structures, and structural characteristics, providing new information about W_2GaX . Because of this, we believe that this work will provide useful guidance for next theoretical and experimental investigations concerning Tungsten-based MAX phases.

2. Computational details

In the current work, the band structures and optical characteristics of W_2GaX were calculated using the WIEN2k code, which is based on the “density functional theory (DFT) based full-potential linearized augmented plane wave (FP-LAPW) method” [35]. This method has established a robust calculation foundation, enabling us to obtain reliable and comprehensive results. The approach employed in this study involves dividing the crystal unit cell into two well-defined regions: the interstitial space and the non-overlapping Muffin-Tin (MT) spheres, each centered around the nucleus of an atom. Specific basis sets are applied within these regions. The atomic wave functions derived from solving the Schrödinger equation with spherical harmonic expansions have been primarily applied within the MT spheres with a radius (R_{MT}). We also utilized a plane wave expansion technique in the space between the MT spheres (interstitial region). We efficiently captured the charge density and potential by integrating a Fourier series in the interstitial region and lattice harmonics inside the MT spheres. This comprehensive method allowed us to gain valuable insights into the wave functions and electronic properties of the W_2GaX . A value of 10 was assigned to l_{max} representing the maximum quantum number, which governs the atomic wave functions within the MT sphere. For the interstitial region, we determined the energy cutoff K_{max} be $8.0/R_{MT}$ for expanding wave functions using plane waves. To ensure accurate calculations and computational efficiency, the charge density underwent a Fourier expansion limited to $G_{max} = 16$. Several tests were conducted to achieve total energy convergence of 10^{-5} Rydberg per unit cell. Our study utilized R_{MT} values of 2.24 atomic units (a.u.) for W, 2.50 a.u. for Ga, 1.74 a.u. for C, 2.02 a.u. for F, and 1.62 a.u. for N atoms. Using a mesh that covered the irreducible wedge of the Brillouin zone with dimensions of $28 \times 28 \times 6$, we employed the augmented tetrahedron method [36] for reciprocal space integration. The “Perdew, Burke, and Ernzerhof (PBE) formulation of the Generalized Gradient Approximation (GGA)” was utilized to handle the “exchange–correlation potential” [37]. The utilized computational method has proven to be reliable enough for conducting electronic structure calculations [38–49]. For calculations of the optical properties of the W_2GaX compounds, the Drude damping, and plasma frequency have been chosen as 0.05 eV and 3 eV. Literature suggests the selected values of the Drude damping and plasma frequency as suitable for MAX phases and other analogous compounds [50–52].

3. Results and discussion

The W_2GaX compounds of 211-MAX phases (shown in Fig. 1) adopt a hexagonal crystal structure where the W atoms are located at $(1/3, 2/3, z)$ atomic coordinates. The $(0, 0, 0)$ and $(1/3, 2/3, 3/4)$ atomic coordinates are occupied by the X and Ga atoms, respectively. The unit cell of these compounds is formed of two formula units and exhibit space group $P6_3/mmc$ (No 194). The W atoms are octahedrally bonded to the X atoms, making a layer of W_6X octahedron along the 001 direction. The W_6X octahedron layer is sandwiched between the Ga atomic layer within the unit cell. The lattice constants of the W_2GaC compound calculated using PBE-GGA amount to $a = b = 3.107$ Å and $c = 11.759$ Å. In the case of W_2GaN , $a = b$ have been recorded as 3.0704 Å and c as 11.849 Å. Similarly, the optimized lattice constants of W_2GaF have been found as $a = b = 3.148$ Å and $c = 14.088$ Å. Unfortunately, we didn't find literature on the lattice parameters of these compounds for comparison of our results. However, these results are comparable to the lattice parameters reported for W_2GeC as $a = b = 3.1437$ [53], 3.351 [54] Å and $c = 12.1600$ [53], 13.943 [54] Å. The slightly larger lattice constants of W_2GaC than W_2GeC can be attributed to the relatively larger ionic radii of Ga (136 pm) than Ge (125 pm).

Using equation 1, we estimated the cohesive energy (E_{coh}) to comprehend the stability of the W_2GaX . In Equation 1 ($E_{W_2GaX}^{211-MAX}$) is the energy of the W_2GaX , whereas E_W , E_{Ga} , and E_X are the energy of the W, Ga, and X atoms respectively.

$$E_{coh} = (E_{W_2GaX}^{211-MAX}) - xE_W - yE_{Ga} - zE_X / (x + y + z) \dots \dots \dots (1).$$

The E_{coh} of W_2GaC , W_2GaN , and W_2GaF obtained through equation 1 equals 7.31, 6.40, and 5.05 eV, respectively. The E_{coh} calculated for W_2GaX 211-MAX phases are matching to 5.20 for Sc_2AlB [55], 4.40 for Y_2AlB [55], 6.09 for Ti_2AlN [56], 7.183 for Ti_2CdC [57], and 6.29 [56] reported for Ti_2AlC respectively.

To evaluate the electronic characteristics of W_2GaX compounds within the MAX phases, we executed calculations for their electronic structures (Fig. 2) and density of states (DOS) (Fig. 3). The analysis reveals that the valence and conduction bands of these MAX phases overlap at the Fermi level, suggesting their metallic nature. The metallic nature of W_2GaX MAX phases agrees with literature which reports that all the MAX phases are metallic [31–33,58]. The metallic nature is mainly caused by the occurrence of W-*d* states that are dispersed with a relatively high density across the electronic structures. Besides W-*d* states, the C-*p* states also demonstrate a considerable density over the Fermi level. However, the C-*p* states demonstrated the highest density at the bottom of the valence band at ~ -5.5 eV. Similarly, the bottom of the

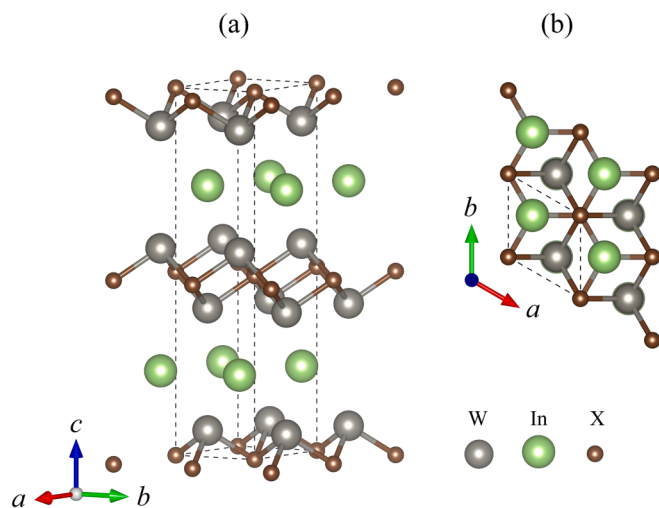


Fig. 1. The depiction of W_2GaX 's crystal structure, with (a) representing the unit cell and (b) displaying the top view.

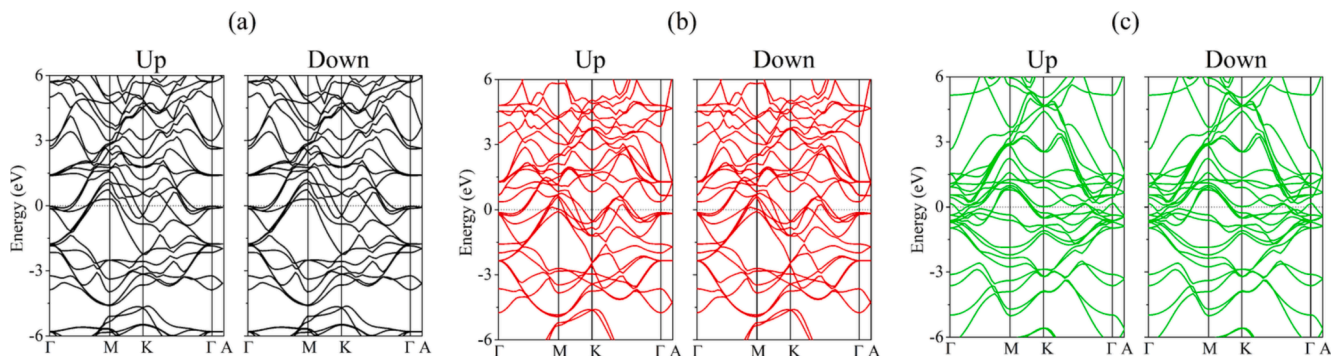


Fig. 2. The depiction of up and down spin electronic structures of (a) W_2GaC , (b) W_2GaN , and (c) W_2GaF .

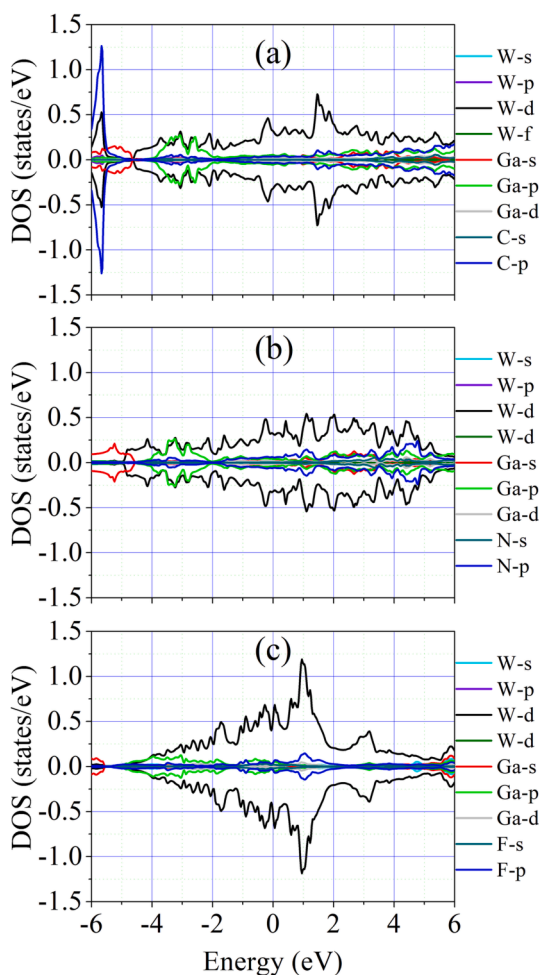


Fig. 3. The spin-polarized DOS illustrations for (a) W_2GaC , (b) W_2GaN , and (c) W_2GaF . The DOS plots for up and down spins are shown along the positive and negative y-axis.

valence band is formed by mixed W-d and Ga-s states. All the three compounds exhibited different arrangements of DOS from each other. However, for each compound, the spin up and down DOS are nearly symmetrical that cancels the effect of opposite spin electrons and thus reduces the magnetic moment of a magnetic material. We accordingly recorded negligible magnetic moments $0.0008 \mu_B$, $0.0002 \mu_B$, and $0.0030 \mu_B$ in the case of W_2GaC , W_2GaN , and W_2GaF , respectively. Therefore, the W_2GaX MAX phases can be inferred as nonmagnetic metallic materials.

In the following section of the article, the optical properties of these

W_2GaX have been discussed in detail. In Fig. 4, the optical reflection, indicates that these materials can reflect more than 60 % of the infrared light. However, the reflection of visible light is reduced to less than 50 % by these W_2GaX MAX phases. Because metallic materials are inherently reflective, the metallic character of these W_2GaX MAX phases accounts for the considerable reflection of the incident infrared and visible light. Fig. 4 illustrates the rapid increase in the reflection of UV light from ~ 7 eV to ~ 10 eV, despite the fact that the reflection of UV light with energy less than ~ 7 eV is greatly decreased. The optical reflection declined again for incident light of energy above ~ 10 eV. These predictions indicate their potential for applications in optical coatings and mirrors.

Like optical reflection, the refraction of infrared light by these W_2GaX MAX phases shown in Fig. 5 is the highest for infrared radiations. In contrast, it has drastically decreased for UV and visible light. For incoming light with an energy of less than 10 eV, the refractive indices stay greater than one. Similarly, it has been observed that for UV light with an energy greater than 10 eV, the optical reflection is minimal. These predictions lead to the hypothesis that the W_2GaX become more opaque to UV light with energies greater than 10 eV.

Our observations of the absorption spectrum depicted in Fig. 6

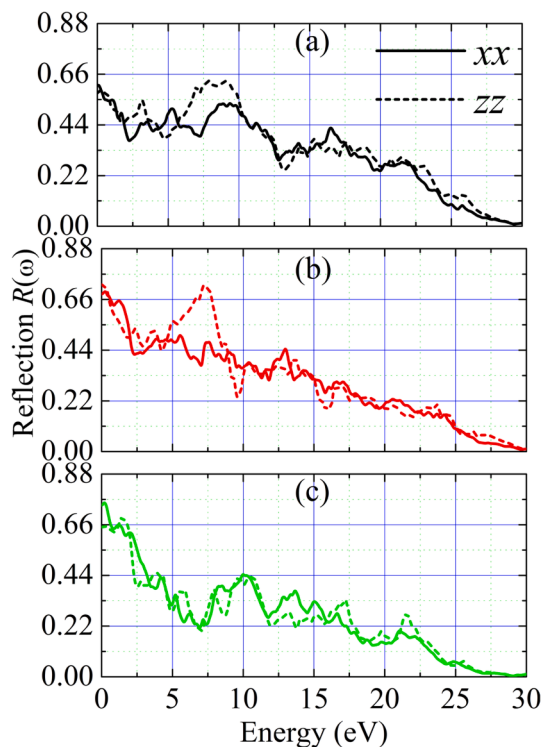


Fig. 4. The schematics of the reflectivity spectrum of (a) W_2GaC , (b) W_2GaN , and (c) W_2GaF .

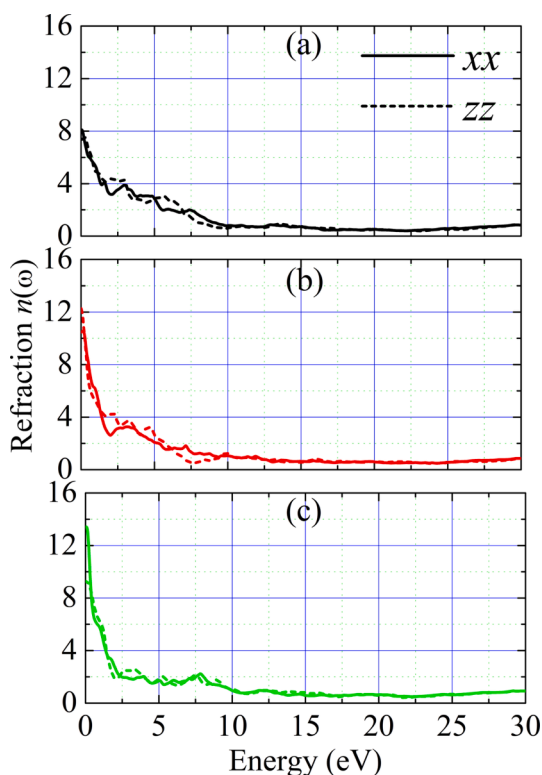


Fig. 5. The schematics of the refraction spectrum of (a) W_2GaC , (b) W_2GaN , and (c) W_2GaF .

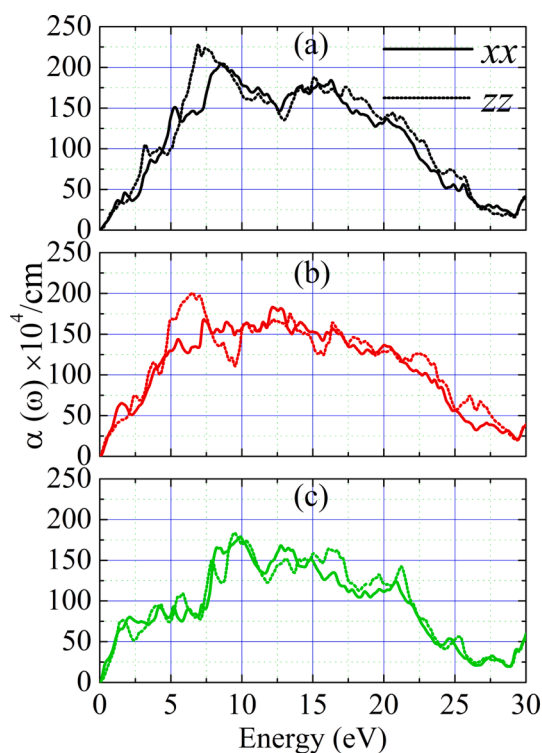


Fig. 6. The schematics of the absorption spectrum of (a) W_2GaC , (b) W_2GaN , and (c) W_2GaF .

further suggest that, while interacting with incident light, the W_2GaX absorbs a substantial part of light during the electronic transition between high and low energy states. In Fig. 6, one can see that, unlike

optical refraction and reflection, the infrared light's absorption is relatively insignificant for the W_2GaX MAX phases. However, the infrared optical absorption threshold suggests that the movement of charge carriers from low to high-energy states can be initiated by even low-energy photons. This capability stems from the gapless electronic configurations of the metallic W_2GaX , enabling electrons to readily move to higher energy states. However, the optical absorption has experienced a dramatic boost for visible light, where the refraction and reflection for these lights have been significantly degraded. Overall, these compounds demonstrated absorption of the order of $\sim 10^4 \text{ cm}^{-1}$ of infrared, $\sim 10^5 \text{ cm}^{-1}$ of visible, and $\sim 10^6 \text{ cm}^{-1}$ of UV light. This shows that the W_2GaX MAX phases have the capability to absorb a broad part of the incident light and, therefore, may find exciting applications in energy harvesting devices.

Fig. 7 illustrates the correlation between W_2GaX 's optical conductivity and photon energy. Exposure of conducting materials to light of appropriate energy induces optical conductivity by elevating electrons from lower to higher energy states, consequently generating an electric current. Interestingly, W_2GaX , because of its metallic nature, shows a threshold optical conductivity when exposed to infrared radiation. As we move towards the visible light region, W_2GaX demonstrates a substantial enhancement in optical conductivity. Consequently, this significant improvement enables the W_2GaX to conduct electricity much more efficiently when exposed to visible light.

The optical conductivity of W_2GaX compounds, specifically W_2GaC and W_2GaN , reaches its peak within the energy range of 4 eV to 6 eV, whereas W_2GaF shows maximum optical conductivity at 2 eV and 8 eV. This indicates their favorable electrical conduction capabilities upon exposure to ultraviolet light. Furthermore, W_2GaX displays anisotropic behavior in its optical conductivity along the x- and z-directions. This suggests that the optical conductivity of W_2GaX may differ based on the orientation of incident light relative to the crystal structure. Comparing different compositions of W_2GaX in Fig. 7, it is found that W_2GaC exhibits the highest optical conductivity when subjected to light, surpassing both W_2GaN and W_2GaF , making it a promising material for

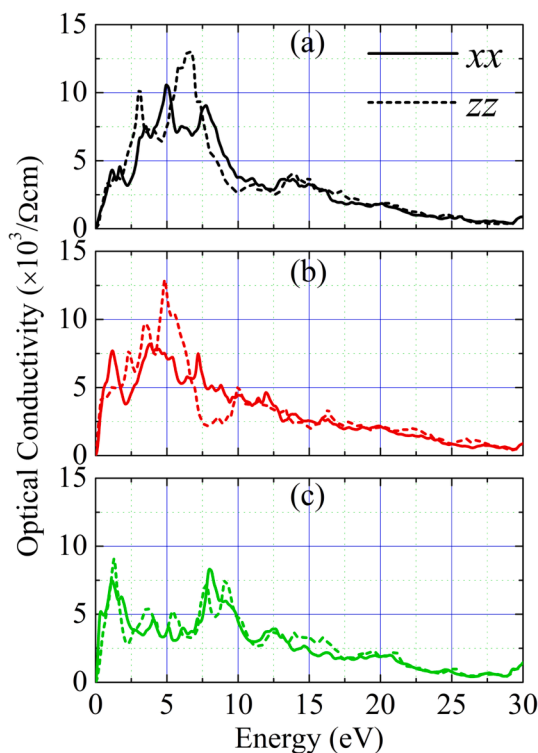


Fig. 7. The schematics of the optical conductivity of (a) W_2GaC , (b) W_2GaN , and (c) W_2GaF .

various conduction applications. The distinct differences in their chemical and electronic band structures account for the variations in their conductive properties. However, as the photon energy surpasses 10 eV, the optical conductivity of the material begins to decline.

Several physical phenomena can elucidate this observed decrease in optical conductivity. One such explanation is that higher-energy photons are more prone to scattering, which ultimately reduces the overall conductivity of W_2GaN and hinders the efficient movement of electrons into the conduction band. The second possibility is the saturation of excited charge carriers. When exposed to high photon energies, numerous electrons are already elevated to higher energy states. As a result, the density of excited carriers, specifically electrons in the conduction band, reaches a saturation threshold. This limits the ability of energy photons to cause a proportional rise in the number of excited carriers, thereby restricting the growth in optical conductivity.

4. Conclusion

In summary, we have investigated the W_2GaX MAX phases using first principles approach, to gain insightful knowledge of their electronic and optical behavior. The cohesive energies calculated for W_2GaC , W_2GaN , and W_2GaF have confirmed their stability and are in excellent agreement with existing literature. The electronic structures of W_2GaX reveal nonmagnetic metallic behavior due to the symmetric dispersion of electron states and may find a variety of electronic applications. Furthermore, the optical properties of W_2GaX MAX phases have been thoroughly explored, indicating that they can reflect and absorb light over a wide wavelength range. These materials have the potential to be used in optical coatings and mirrors due to their capacity to reflect more than 60 % infrared radiation and up to 50 % visible light. Furthermore, the significant absorption of infrared, visible, and UV light with high absorption coefficients suggests that they could be used in energy harvesting and sensing technologies. Additionally, W_2GaC has the highest optical conductivity among the investigated compounds, making it a promising candidate for advanced conduction applications. Our present study provides a comprehensive understanding of the physical behaviors exhibited by the novel W_2GaX -based MAX phase, thus serving as a useful guide for upcoming theoretical and experimental research.

CRedit authorship contribution statement

Bakhtiar Ul Haq: Conceptualization, Investigation, Writing – original draft, Writing – review & editing. **Se-Hun Kim:** Resources, Software, Supervision, Validation. **R. Ahmed:** Supervision, Validation, Writing – review & editing. **Aijaz Rasool Chaudhry:** . **Muhammad Shabbir:** Methodology, Resources, Validation. **A. Laref:** Supervision, Validation.

Declaration of competing interest

The authors declare that they have no known competing financial interests or personal relationships that could have appeared to influence the work reported in this paper.

Data availability

Data will be made available on request.

Acknowledgment

This work is supported by the Brain Pool program (No. 2022H1D3A2A02063677) and "Regional Innovation Strategy (RIS)" (No. 2023RIS-009) through the National Research Foundation of Korea (NRF). A. R. Chaudhry is thankful to the Deanship of Scientific Research at the University of Bisha for supporting this work through the Fast-Track Research Support Program. The author (Muhammad Shabbir)

extends his appreciation to the Research Center for Advanced Materials Science at King Khalid University for funding the work under grant number RCAMS/KKU/027-23.

References

- [1] M.W. Barsoum, The MN+ 1AXN phases: A new class of solids: Thermodynamically stable nanolaminates, *Prog. Solid State Chem.* 28 (1–4) (2000) 201–281.
- [2] M.A. Rahman, I. Kholil, R. Khatun, S. Sarker, M. Hasan, M.A. Ali, M.Z. Rahaman, K. M. Hossain, M.I. Haque, M.Z. Hasan, High pressure study of new type of MAX phases: Hf_2AB_2 (A = In, Sn), *Physica Status Solidi (b)*, 2022.
- [3] M. Khazaei, A. Ranjbar, K. Esfarjani, D. Bogdanovski, R. Dronskowski, S. Yunoki, Insights into exfoliation possibility of MAX phases to MXenes, *PCCP* 20 (13) (2018) 8579–8592.
- [4] M. Khazaei, M. Arai, T. Sasaki, M. Estili, Y. Sakka, The effect of the interlayer element on the exfoliation of layered Mo_2AC (A = Al, Si, P, Ga, Ge, As or In) MAX phases into two-dimensional Mo_2C nanosheets, *Sci. Technol. Adv. Mater.* 15 (1) (2014), 014208.
- [5] B.U. Haq, S.-H.K., S. AlFaify, S.A. Tahir, R. Ahmed, A. Samah Al-Qaisi, Laref, Investigations of the electronic and optical properties of V_2InC and V_2InN based MAX phases in the framework of density functional theory, *Solid State Commun.* 377 (2024), 115388.
- [6] M. Cover, O. Warschkow, M. Bilek, D. McKenzie, A comprehensive survey of M_2AX phase elastic properties, *J. Phys. Condens. Matter* 21 (30) (2009), 305403.
- [7] M. Khazaei, M. Arai, T. Sasaki, M. Estili, Y. Sakka, Trends in electronic structures and structural properties of MAX phases: a first-principles study on M_2AlC (M = Sc, Ti, Cr, Zr, Nb, Mo, Hf, or Ta), M_2AlN , and hypothetical M_2AlB phases, *J. Phys. Condens. Matter* 26 (50) (2014), 505503.
- [8] Z. Sun, S. Li, R. Ahuja, J.M. Schneider, Calculated elastic properties of M_2AlC (M = Ti, V, Cr, Nb and Ta), *Solid State Commun.* 129 (9) (2004) 589–592.
- [9] J. Hettinger, S. Lofland, P. Finkel, T. Meehan, J. Palma, K. Harrell, S. Gupta, A. Ganguly, T. El-Raghy, M. Barsoum, Electrical transport, thermal transport, and elastic properties of M_2AlC (M = Ti, Cr, Nb, and V), *Phys. Rev. B* 72 (11) (2005), 115120.
- [10] M. Ali, M. Hossain, M. Uddin, A. Islam, D. Jana, S. Naqib, DFT insights into new B-containing 212 MAX phases: Hf_2AB_2 (A = In, Sn), *J. Alloy. Compd.* 860 (2021), 158408.
- [11] Barsoum, M.W., *MAX phases: properties of machinable ternary carbides and nitrides*. 2013: John Wiley & Sons.
- [12] X. Wang, Y. Zhou, Layered machinable and electrically conductive Ti_2AlC and Ti_3AlC_2 ceramics: a review, *J. Mater. Sci. Technol.* 26 (5) (2010) 385–416.
- [13] J.-C. Nappé, P. Grosseau, F. Audubert, B. Guilhot, M. Beauvy, M. Benabdesselam, I. Monnet, Damages induced by heavy ions in titanium silicon carbide: Effects of nuclear and electronic interactions at room temperature, *J. Nucl. Mater.* 385 (2) (2009) 304–307.
- [14] M.M. Ali, M. Hadi, I. Ahmed, A. Haider, A. Islam, Physical properties of a novel boron-based ternary compound Ti_2InB_2 , *Mater. Today Commun.* 25 (2020), 101600.
- [15] M.W. Barsoum, T. El-Raghy, The MAX phases: Unique new carbide and nitride materials: Ternary ceramics turn out to be surprisingly soft and machinable, yet also heat-tolerant, strong and lightweight, *Am. Sci.* 89 (4) (2001) 334–343.
- [16] M. Ali, M. Hadi, M. Hossain, S. Naqib, A. Islam, Theoretical investigation of structural, elastic, and electronic properties of ternary boride $MoAlB$, *Physica Status Solidi (b)* 254 (7) (2017) 1700010.
- [17] S. Kota, M. Sokol, M.W. Barsoum, A progress report on the MAB phases: atomically laminated, ternary transition metal borides, *Int. Mater. Rev.* 65 (4) (2020) 226–255.
- [18] M. Hadi, Superconducting phases in a remarkable class of metallic ceramics, *J. Phys. Chem. Solid* 138 (2020), 109275.
- [19] M. Ade, H. Hillebrecht, Ternary borides Cr_2AlB_2 , Cr_3AlB_4 , and Cr_4AlB_6 : The first members of the series $(CrB_2)_n$ $CrAl$ with $n = 1, 2, 3$ and a unifying concept for ternary borides as MAB-phases, *Inorg. Chem.* 54 (13) (2015) 6122–6135.
- [20] A.J. Mannix, X.-F. Zhou, B. Kiraly, J.D. Wood, D. Alducin, B.D. Myers, X. Liu, B. L. Fisher, U. Santiago, J.R. Guest, Synthesis of borophenes: Anisotropic, two-dimensional boron polymorphs, *Science* 350 (6267) (2015) 1513–1516.
- [21] M.W. Barsoum, T. El-Raghy, Synthesis and characterization of a remarkable ceramic: Ti_3SiC_2 , *J. Am. Ceram. Soc.* 79 (7) (1996) 1953–1956.
- [22] W. Jeitschko, H. Nowotny, Die kristallstruktur von Ti_3SiC_2 —ein neuer komplexkarbid-typ, *Monatshefte Für Chemie-Chemical Monthly* 98 (2) (1967) 329–337.
- [23] W. Jeitschko, H. Nowotny, F. Benesovsky, Carbides of formula T_2MC , *Journal of the Less Common Metals* 7 (2) (1964) 133–138.
- [24] S. Geller, R. Grant, U. Gonser, Crystal chemistry and magnetic structures of substituted Ca_2FeO_5, *Prog. Solid State Chem.* 5 (1971) 1–26.
- [25] M. Sokol, V. Natu, S. Kota, M.W. Barsoum, On the chemical diversity of the MAX phases, *Trends in Chemistry* 1 (2) (2019) 210–223.
- [26] X. Li, J. Malzbender, G. Yan, J. Gonzalez-Julian, R. Schwaiger, A combined experimental and modeling study revealing the anisotropic mechanical response of Ti_2AlN MAX phase, *J. Eur. Ceram. Soc.* 41 (12) (2021) 5872–5881.
- [27] P. Eklund, M. Beckers, U. Jansson, H. Högberg, L. Hultman, The Mn+ 1AXn phases: Materials science and thin-film processing, *Thin Solid Films* 518 (8) (2010) 1851–1878.

- [28] B.U. Haq, S.-H. Kim, S. Tahir, R. Ahmed, S. AlFaify, K. Alam, A.R. Chaudhry, Theoretical investigations of O-and F-surface functionalization of MXenes based on Cr₂M (M= C, N), Mater. Sci. Semicond. Process. 168 (2023), 107837.
- [29] B.U. Haq, S.-H. Kim, S. AlFaify, M.A. Javed, R. Ahmed, K. Alam, A.R. Chaudhry, Physical Properties 211-type of MAX Phases based on Mn₂AlX (X= C, N, and F) through First-Principles Approaches, Materials Today Communications 37 (2023) 107384.
- [30] M.A. Hadi, M. Akhter, M.S. Ahasan, I. Ahmed, M.A. Kashem, Realization of diversity in physical properties of Zr₂Se (B1-xSex) MAX phases through DFT approach, J. Am. Ceram. Soc. 106 (10) (2023) 6177–6193.
- [31] W. Zhou, L. Liu, P. Wu, First-principles study of structural, thermodynamic, elastic, and magnetic properties of Cr₂GeC under pressure and temperature, J. Appl. Phys. 106 (3) (2009), 033501.
- [32] A.S. Ingason, A. Mockute, M. Dahlqvist, F. Magnus, S. Olafsson, U.B. Arnalds, B. Alling, I.A. Abrikosov, B. Hjörvarsson, P.Å. Persson, Magnetic self-organized atomic laminate from first principles and thin film synthesis, Phys. Rev. Lett. 110 (19) (2013), 195502.
- [33] M. Dahlqvist, B. Alling, I. Abrikosov, J. Rosén, Magnetic nanoscale laminates with tunable exchange coupling from first principles, Phys. Rev. B 84 (22) (2011), 220403.
- [34] R. Meshkian, M. Dahlqvist, J. Lu, B. Wickman, J. Halim, J. Thörnberg, Q. Tao, S. Li, S. Intikhab, J. Snyder, W-based atomic laminates and their 2D derivative W₁. 33C MXene with vacancy ordering, Adv. Mater. 30 (21) (2018) 1706409.
- [35] K. Schwarz, P. Blaha, Solid state calculations using WIEN2k, Comput. Mater. Sci 28 (2) (2003) 259–273.
- [36] P.E. Blöchl, Projector Augmented-Wave Method, Physical Review B 50 (24) (1994) 17953.
- [37] J.P. Perdew, K. Burke, M. Ernzerhof, Generalized gradient approximation made simple, Phys. Rev. Lett. 77 (18) (1996) 3865.
- [38] B. Ul Haq, A. Afaq, R. Ahmed, S. Naseem, A comprehensive DFT study of zinc oxide in different phases, Int. J. Mod. Phys. C 23 (06) (2012) 1250043.
- [39] S. Shabbir, A. Shaari, B.U. Haq, R. Ahmed, M. Ahmed, Investigations of novel polymorphs of ZnO for optoelectronic applications, Optik 206 (2020), 164285.
- [40] S.U. Rehman, F.K. Butt, F. Hayat, B.U. Haq, Z. Tariq, F. Aleem, C. Li, An insight into a novel cubic phase SnSe for prospective applications in optoelectronics and clean energy devices, J. Alloy. Compd. 733 (2018) 22–32.
- [41] B.U. Haq, S. AlFaify, A. Laref, R. Ahmed, F.K. Butt, A.R. Chaudhry, S.U. Rehman, Q. Mahmood, Optoelectronic properties of new direct bandgap polymorphs of single-layered Germanium sulfide, Ceram. Int. 45 (14) (2019) 18073–18078.
- [42] B.U. Haq, S. AlFaify, A. Laref, Design and characterization of novel polymorphs of single-layered tin-sulfide for direction-dependent thermoelectric applications using first-principles approaches, PCCP 21 (8) (2019) 4624–4632.
- [43] B.U. Haq, S. AlFaify, T. Al-shahrani, S. Al-Qaisi, R. Ahmed, A. Laref, S. Tahir, First-principles investigations of ZnO monolayers derived from zinc-blende and 5–5 phases for advanced thermoelectric applications, J. Phys. Chem. Solid 149 (2021), 109780.
- [44] B.U. Haq, S. AlFaify, T. Alshahrani, R. Ahmed, F.K. Butt, S.U. Rehman, Z. Tariq, Devising square-and hexagonal-shaped monolayers of ZnO for nanoscale electronic and optoelectronic applications, Sol. Energy 211 (2020) 920–927.
- [45] B.U. Haq, S. AlFaify, T.A. Alrebdi, R. Ahmed, S. Al-Qaisi, M. Taib, G. Naz, S. Zahra, Investigations of optoelectronic properties of novel ZnO monolayers: A first-principles study, Mater. Sci. Eng. B 265 (2021), 115043.
- [46] B.U. Haq, S. AlFaify, R. Ahmed, A. Laref, Q. Mahmood, E. Algrafy, Optoelectronic properties of PbSe monolayers from first-principles, Appl. Surf. Sci. 525 (2020), 146521.
- [47] B.U. Haq, R. Ahmed, A. Shaari, N. Ali, Y. Al-Douri, A. Reshak, Comparative study of Fe doped ZnO based diluted and condensed magnetic semiconductors in wurtzite and zinc-blende structures by first-principles calculations, Mater. Sci. Semicond. Process. 43 (2016) 123–128.
- [48] B.U. Haq, R. Ahmed, J.Y. Rhee, A. Shaari, S. AlFaify, M. Ahmed, Composition-induced influence on the electronic band structure, optical and thermoelectric coefficients of the highly mismatched GaNSb alloy over the entire range: a DFT analysis, J. Alloy. Compd. 693 (2017) 1020–1027.
- [49] B.U. Haq, A. Afaq, R. Ahmed, S. Naseem, Structural, electronic, and magnetic properties of Co-doped ZnO, Chin. Phys. B 21 (9) (2012), 097101.
- [50] M. Hadi, R. Vovk, A. Chroneos, Physical properties of the recently discovered Zr₂ (Al_{1-x}Bi_x)C MAX phases, J. Mater. Sci. Mater. Electron. 27 (2016) 11925–11933.
- [51] M. Hadi, M. Roknuzzaman, M. Nasir, U. Monira, S. Naqib, A. Chroneos, A. Islam, J. A. Alarco, K. Ostrikov, Effects of Al substitution by Si in Ti₃AlC₂ nanolaminate, Sci. Rep. 11 (1) (2021) 3410.
- [52] M. Hadi, N. Kelaidis, P.-P. Filippatos, S.-R. Christopoulos, A. Chroneos, S. Naqib, A. Islam, Optical response, lithiation and charge transfer in Sn-based 211 MAX phases with electron localization function, J. Mater. Res. Technol. 18 (2022) 2470–2479.
- [53] A. Bouhemadou, Calculated structural, electronic and elastic properties of M₂GeC (M= Ti, V, Cr, Zr, Nb, Mo, Hf, Ta and W), Appl. Phys. A 96 (4) (2009) 959–967.
- [54] M.B. Kanoun, S. Goumri-Said, A.H. Reshak, A.E. Merad, Electro-structural correlations, elastic and optical properties among the nanolaminated ternary carbides Zr₂AC, Solid State Sci. 12 (5) (2010) 887–898.
- [55] S. Aydin, 211-MAX borides: The stable boron-substituted 211-MAX compounds by first-principles, Mater. Today Commun. 25 (2020), 101689.
- [56] I. Shein, A. Ivanovskii, Graphene-like titanium carbides and nitrides Tin+ 1Cn, Tin + 1Nn (n= 1, 2, and 3) from de-intercalated MAX phases: First-principles probing of their structural, electronic properties and relative stability, Comput. Mater. Sci 65 (2012) 104–114.
- [57] Y. Bai, X. He, M. Li, Y. Sun, C. Zhu, Y. Li, Ab initio study of the bonding and elastic properties of Ti₂CdC, Solid State Sci. 12 (1) (2010) 144–147.
- [58] B. Ul Haq, M.M. Alsardia, I.B. Khadka, R. Ahmed, S. AlFaify, F.K. Butt, Z. Ali Shah, S.-H. Kim, First-Principles Study of the Physical Properties of Ti₂SnX 568: (2023) 111850. X: C, N) based 211-MAX phases.